bias
Bremer Institut für
angewandte Strahltechnik

F. Vollertsen, J. Sakkiettibutra (Eds.)

Thermal Forming and Welding Distortion

Proceedings of the IWOTE'08:
International Workshop on
Thermal Forming and Welding Distortion

Bremen, Germany, April 22-23, 2008

Thermal Forming and Welding Distortion
Frank Vollertsen, Jens Sakkiettibutra (Eds.)

Strahltechnik Volume 31, BIAS Verlag, Bremen, 2008
Editor of the series: F. Vollertsen

ISBN: 978-3-933762-23-8

Print: DiguPrint Digitaldruck- und Offsetdruck-Service, Bochum
Printed in Germany

Analysis of Deformations Induced by a Laser Beam Pulse

Jacek Widłaszewski

Institute of Fundamental Technological Research of the Polish Academy of Sciences,
Ul. Świętokrzyska 21, Warsaw, 00-048, Poland

Pulsed laser heating is industrially applied in manufacturing processes to produce precise deformation of metal objects. Research on deformations resulting from heating the metal with a stationary heat source is of fundamental importance to comprehend and control thermal forming with a moving heat source. Deformations of a cantilever beam due to pulsed laser heating are experimentally and numerically analyzed in the paper. Samples made of 18-8 type stainless steel were heated with Nd:YAG laser beam. Transient and permanent angular deformation of samples was measured optically with a laser scan micrometer. Uncoupled thermal-mechanical analysis was performed using a three-dimensional finite element method model. Experimentally validated simulations revealed mixed mechanism of deformation consisting of the upsetting mechanism with a contribution of the temperature gradient mechanism.

1 Introduction

Understanding deformations induced by laser pulse heating is a problem of considerable theoretical and practical interest. Local pulsed heating of materials is widely applied in fundamental and applied research of many science disciplines, and in different areas of manufacturing. Pulsed laser heating has been industrially applied since 1980's in positioning of contacts in electric relays [1]. Study of deformations resulting from single pulse heating with a stationary heat source is of fundamental importance to comprehend and control thermal forming with sequences of pulses and/or a moving heat source.

Dependent on laser processing parameters, the part topology and dimensions different shape changes are produced by pulsed local heating of the material. Bending deformation usually is produced when: (1) plastic strains result from steep temperature gradient in the material thickness direction, or (2) the heated region undergoes thermal buckling. The latter phenomenon occurs if the heated region is slender and sufficiently rigidly supported to constrain its thermal expansion. Homogeneous upsetting across the thickness also requires constrains, but no temperature gradient in the thickness direction. Mixed deformation patterns may occur in industrial applications due to actual processing conditions and part geometry.

Experimental and numerical studies on pulsed laser bending have been reported by several researchers. Lee and Lin (2002) investigated deformation of a 304 stainless steel plate heated with a line-shaped CO_2 laser beam [2]. Wang et al. (2005) presented research on dynamic micro-deformations of cantilever beams made of St14 and C45 steels and heated with a CO_2 laser beam of Gaussian intensity distribution [3]. Hsieh and Lin (2004) analysed transient deformation and vibrations caused by pulsed heating of a cantilever beam [4]. Effect of pulse-induced melting and solidification of 301 stainless steel during laser bending was investigated by Zhang and Xu (2004) using a two-dimensional (2D) finite element method (FEM) model [5]. The authors analysed also

pulsed laser bending of silicon microcantilevers modelled in 2D [6]. Differences between experimental and numerical results they explained by simplifications introduced in the 2D model.

This paper presents experimental results and 3D FEM model developed to study micro deformations of a cantilever beam locally heated with a Nd:YAG laser beam and relatively long pulse duration.

2 Experiments

Samples of dimensions 50 x 4.05 x 0.55 mm made of 18-8 type stainless steel were heated with a Nd:YAG laser beam (**figure 1**). They were clamped at one end as cantilever beams.

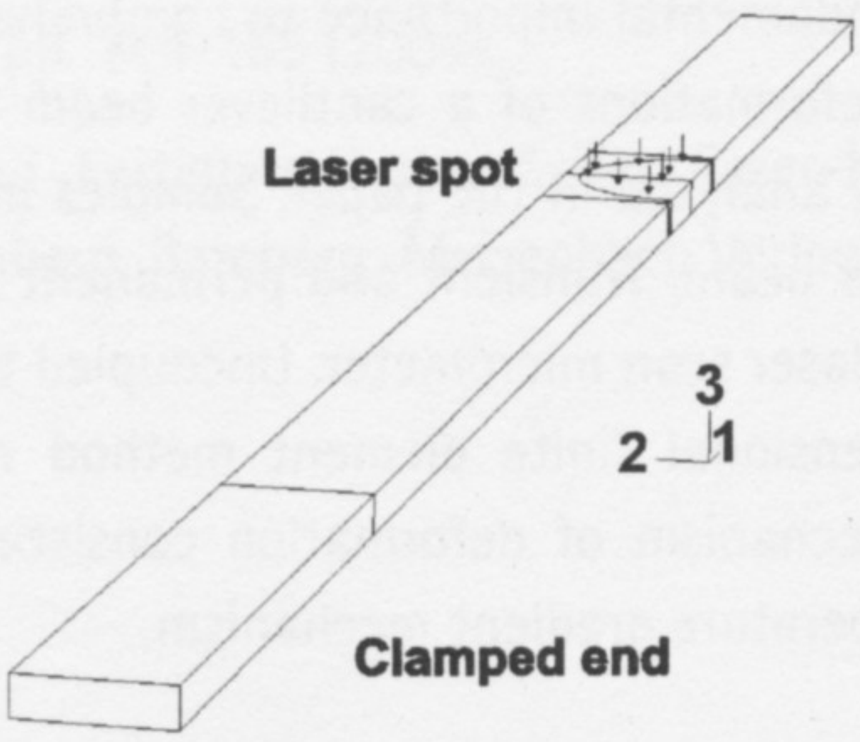

Figure 1: Schematic of experiments - cantilever beam heated with a laser beam. View of a half of symmetric specimen

Nd:YAG laser beam was defocussed to obtain a spot of diameter 3.6 mm on the material surface. Laser operated in the continuous wave (CW) mode. Temperature of specimens was checked with a contact sensor before each laser heating in order to maintain constant initial material temperature (the ambient temperature) for each experiment.

Displacement of an additional light-weight element attached to the free end of the sample was continuously measured with a laser scanning micrometer (Keyence). Angle α of bending deformation induced by the laser pulse was calculated from the linear vertical displacement optically measured with the micrometer. The following formula was used: $\alpha = arctg(u_3 / r)$, where u_3 is the measured displacement in the vertical direction 3 (**figure 1**), r is a distance from the center of laser spot to the measurement location ($r = 48.8$ mm). Accuracy of the applied laser micrometer depends on a number of averaged scans of frequency 400 Hz. Dynamic deformation during heating stage was measured using 16 scans for averaging. To achieve highest measurement accuracy of final angular deformation (after the sample cooled down), the number of averaged scans was switched to 1024 at the end of the cooling stage. Samples were annealed before experiments in a furnace in 400°C for a half an hour in order to reduce initial residual stresses and to increase coupling of laser power due to created oxide layers.

Some examples of experimental results are presented in **figures 2** and **3**. In a series of experiments samples were heated with the same pulse duration 1.05 s and laser power 21, 36.2, 46.3, 59 and 72 W. Resulting final angular deformations of samples are shown in **figure 3**.

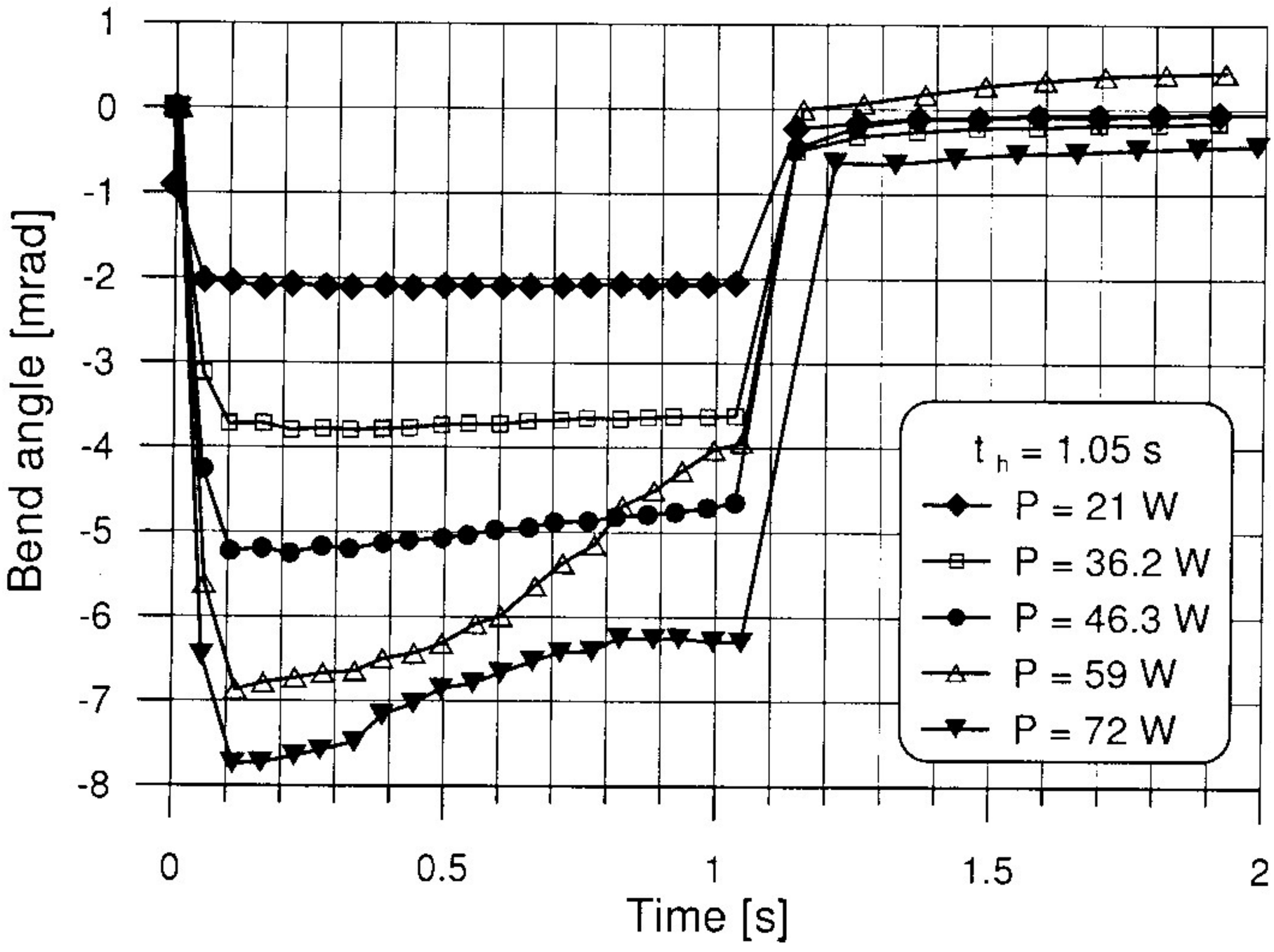

Figure 2: Bend angle variation in experiments with different levels of laser pulse power P and a constant pulse duration t_h 1.05 s

Time runs of the bend angle during laser heating reflect progress of thermally induced deformation. Temperature gradient in the thickness direction induces bending with negative angular deformation and the amplitude dependent on the applied laser power. Deformations produced with pulses of power 21 W and 36.2 W can be regarded as practically thermo-elastic.

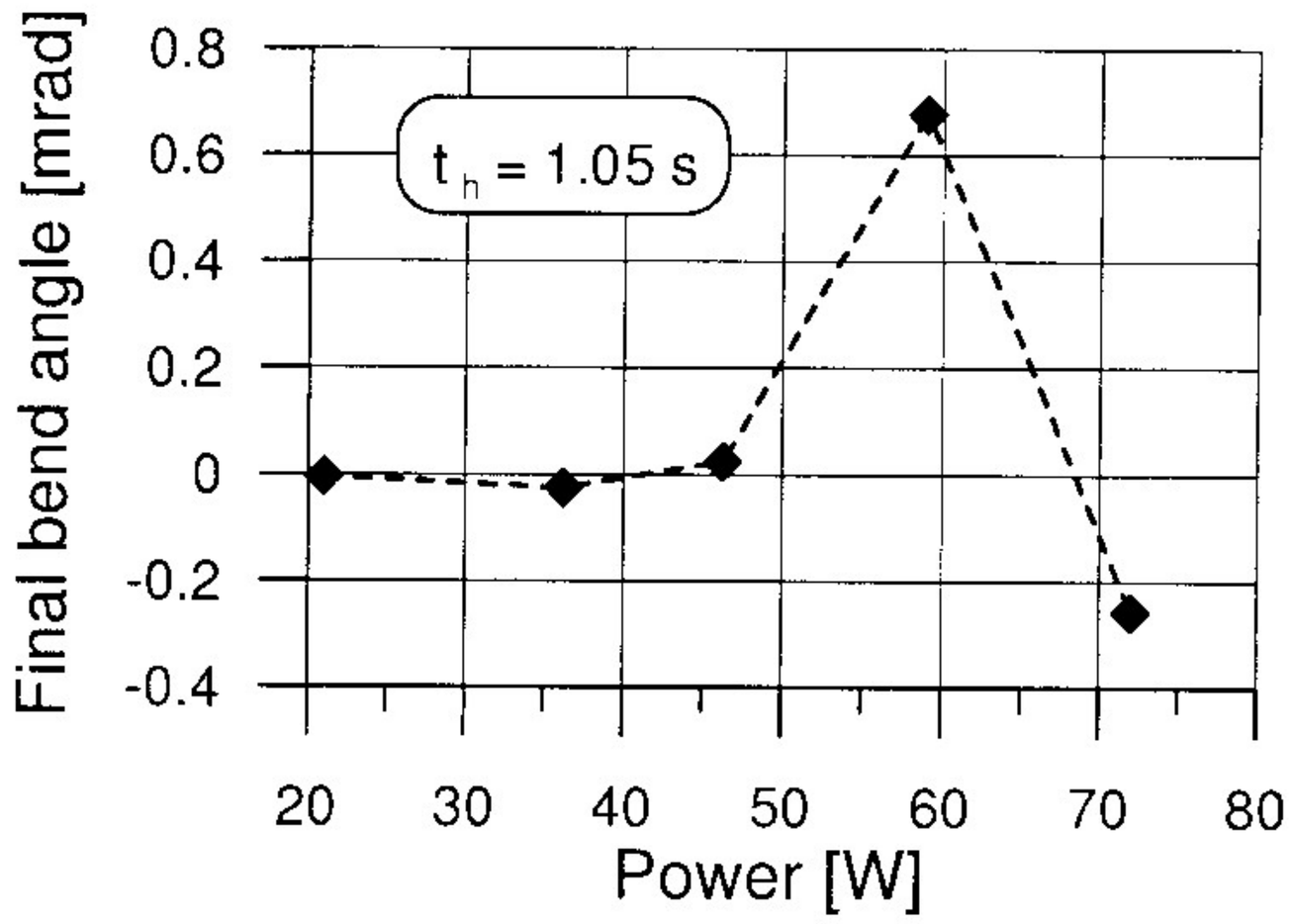

Figure 3: Final angular deformation of specimens heated with different levels of laser pulse power P and a constant pulse duration t_h 1.05 s

Increasing the laser power further we approach thermoplastic deformations, as can be seen for the case of laser power 46.3 W. While the very small positive final bend angle (**figure 3**) one can neglect, as it is close to the measurement resolution, the slope of the bend angle time run, shown in **figure 2**, distinctly indicates a change in the material behavior. Pulsed heating with power 59 W produced definite positive final angular deformation of the specimen. The corresponding bend angle time run presented in **figure 2** clearly differs from experimental data obtained for other cases. The biggest slope of the experimental curve is related to the development of significant

plastic deformation of the sample. The last case of pulsed heating with laser power 72 W is characterized by the negative final angular deformation.

Two parameters are used to characterize fundamental deformation mechanisms in thermal forming: the Fourier similarity number Fo and the ratio of dimension describing extend of the heated area to the material thickness. The Fourier number is a dimensionless time, which allows the Fourier's heat conduction equation to be expressed in a dimensionless form. On the other hand, the Fourier number can be expressed as $Fo = t_h / t_d$, where t_h is the time of heat input into the material and t_d is the characteristic time of heat diffusion. For the case of pulsed heating with a source which is stationary with respect to the material, time t_h is simply the pulse duration. The characteristic time t_d of heat diffusion can be assumed using the solution of the one-dimensional heat conduction problem for a semi-infinite solid subject to constant heat flux on its boundary [7]. The resulting formula $t_d = h^2 / (\kappa)$, where κ is the thermal diffusivity of the body, corresponds to an increase of the body temperature at a distance h to approximately 35% of the surface temperature increase. Applying distance h equal the thickness of a sample we arrive at well known form $Fo = \kappa t_h / h^2$. Using $\kappa = 5.5$ mm^2/s for the stainless steel in the mean process temperature 500°C we get $Fo = 19$ for pulse duration $t_h = 1.05$ s. This value hardly satisfies the condition of a small Fourier number value [8], [9] for the temperature gradient mechanism [10] to be dominating in the case of a moving heat source, neither it is close to the optimal Fourier number value 0.837, as derived in [11]. If we calculate the ratio of the laser spot dimension to the sample thickness we obtain value of 6.5, which corresponds to a transition between the temperature gradient mechanism and the buckling mechanism for the moving heat source [9]. In order to get insight into mechanism of the considered laser pulse induced deformation numerical simulations were performed.

3 Numerical modeling

Numerical simulations were conducted using the finite element method. The following assumptions were made for the numerical modeling. The dependence of temperature on stress and strain was neglected in the problem under consideration, since heat generated due to material deformation is negligible in comparison to the heat delivered by the laser beam. Hence, thermal-mechanical analysis could be decoupled and conducted in two separate steps: (1) determination of temperature field under prescribed heat load and boundary conditions, and (2) elastic-plastic incremental analysis of stress and strain due to the calculated temperature field. Computational domain described one half of the specimen (**figure 1** and 4), taking advantage of the symmetry of the problem with regard to geometry, boundary conditions and heat load.

The power density distribution of the multimode laser beam was approximated by a top-hat model of constant intensity across the laser spot (**figure 4b**). Energy input from the laser beam was modeled as a surface heat source, since the absorption of infrared radiation by metals is confined typically to a thin layer of several tens of nanometers thickness.

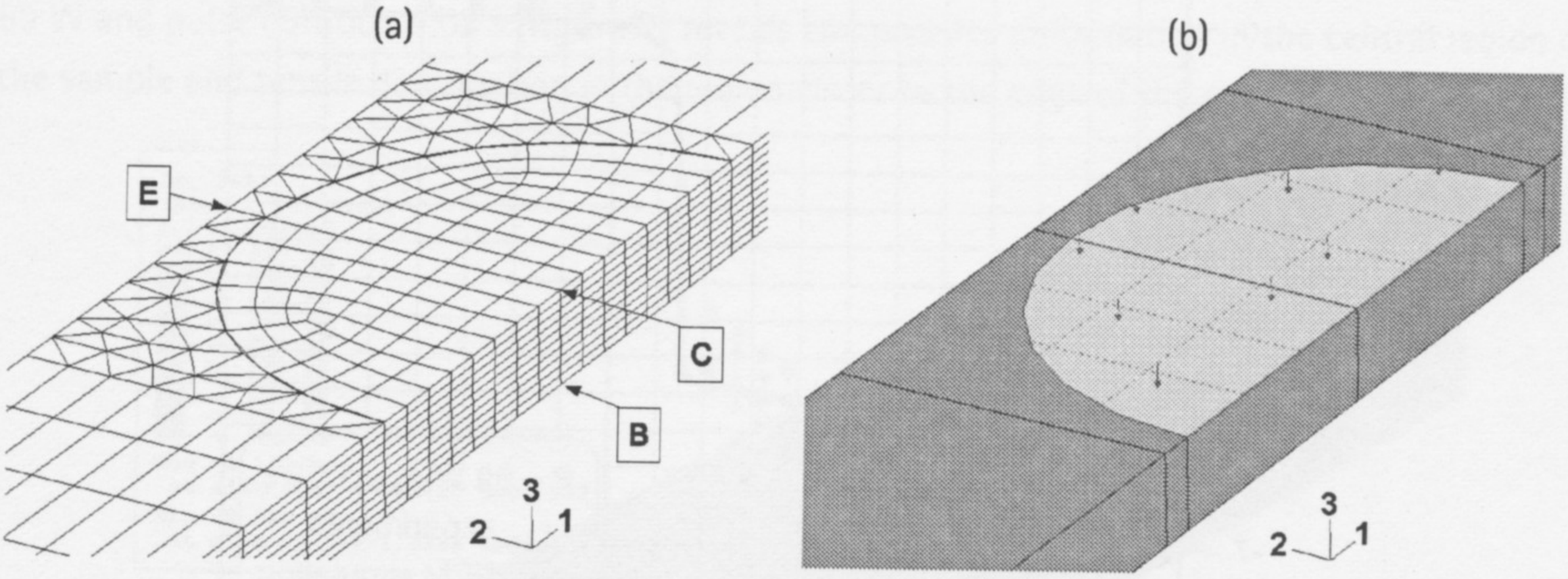

Figure 4: Numerical model: (a) mesh of elements in the laser spot region, (b) the laser spot

Thermal dependences of the following material properties were taken into consideration: thermal conductivity, specific heat, thermal expansion coefficient, Young's modulus, yield stress, Poisson's ratio and density [4], [12], [13], [14], [15]. Constant value of the laser radiation absorption coefficient $A = 0.85$ was employed in calculations. Consequently material emissivity value $\varepsilon = 0.85$ also was used as independent of material temperature. Heat dissipation through free convection described by the Newton's law was applied, with the heat convection coefficient value of 10 W/(m^2 K). Some numerical simulations and sensitivity analysis showed that the values of emissivity and heat convection coefficient play minor role in the considered problem. Therefore their dependence on temperature could also be neglected.

Symmetry condition in the thermal problem was accounted for by considering the plane of symmetry as adiabatic, whereas heat convection and radiation was allowed on all other surfaces of the model. Mechanical symmetry was modeled assuming all points in the plane of symmetry to have no displacement out of this plane. Rigid translation of the model was excluded by fixing one point at the clamped end of the sample. Rigid rotations were prevented assuming two other points in the fixture plane to have no move out of this plane.

The Huber-Mises-Hencky yield criterion was used in thermal-mechanical simulations. Elastic-perfectly plastic isotropic material model was applied. Material hardening was neglected, as plastic deformation occurs mainly in high temperature, where strengthening is substantially reduced by dynamic recovery processes.

Numerical simulations of the three-dimensional problem were performed using ABAQUS software. The same mesh model was used for thermal and mechanical analysis. Three-dimensional linear elements with 6 and 8 nodes were used: wedge elements DC3D6 and hexahedral DC3D8 for thermal problem, and compatible elements C3D6 and C3D8 for mechanical problem. Ten layers of elements were applied in the thickness direction of the specimen in order to accurately model thermal gradient and bending effect. The model consisted of 4380 elements and 4895 nodes.

Figures 5 and **6** present examples of experimental and numerical results of bending angle variation during heating stage and shortly afterwards for the applied laser power 59 W with pulse duration 1.05 s, and power 90 W with pulse duration 0.35 s, respectively.

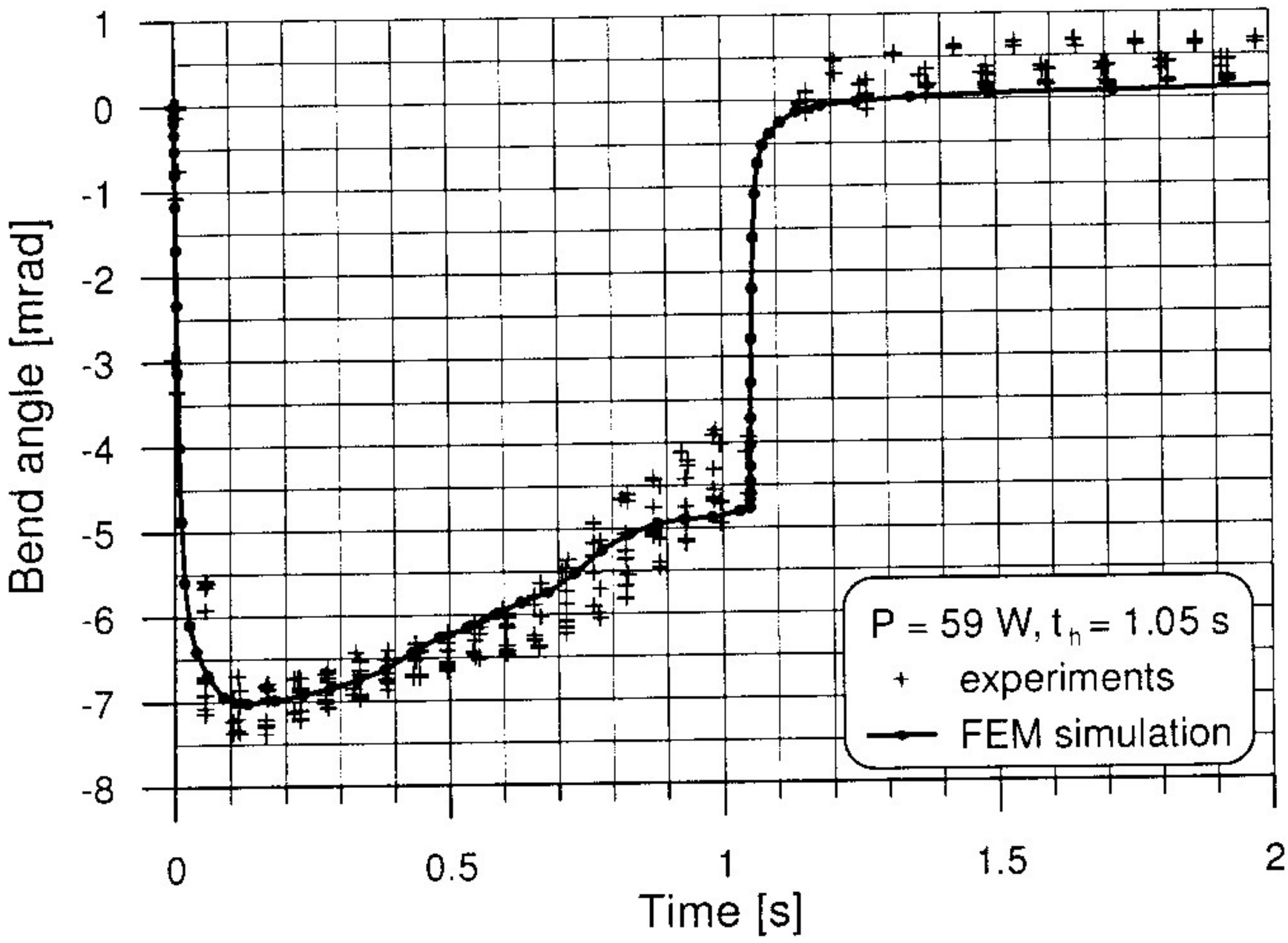

Figure 5: Experimental and numerical bend angle time runs for laser power 59 W and pulse duration 1.05 s

Measurement data for several repetitions of experiments are shown to illustrate the scatter of experimental data due to fluctuations in laser beam power and realized time of pulse duration, initial sample state and measuring accuracy. Fluctuations of the laser beam power can be estimated as ±5% of the nominal value. Accuracy of pulse time duration is approximately ±0.05 s in the experimental setup used.

Taking into account differences between available material data, particularly for thermal expansion coefficient, Young's modulus and yield stress in high temperature, and sensitivity of numerical results to these data, a relatively good agreement with experimental results was achieved. Comparison of experimental and calculated time runs of the bend angle is considered as validation of simulations for detailed analysis of the deformation mechanism in considered cases.

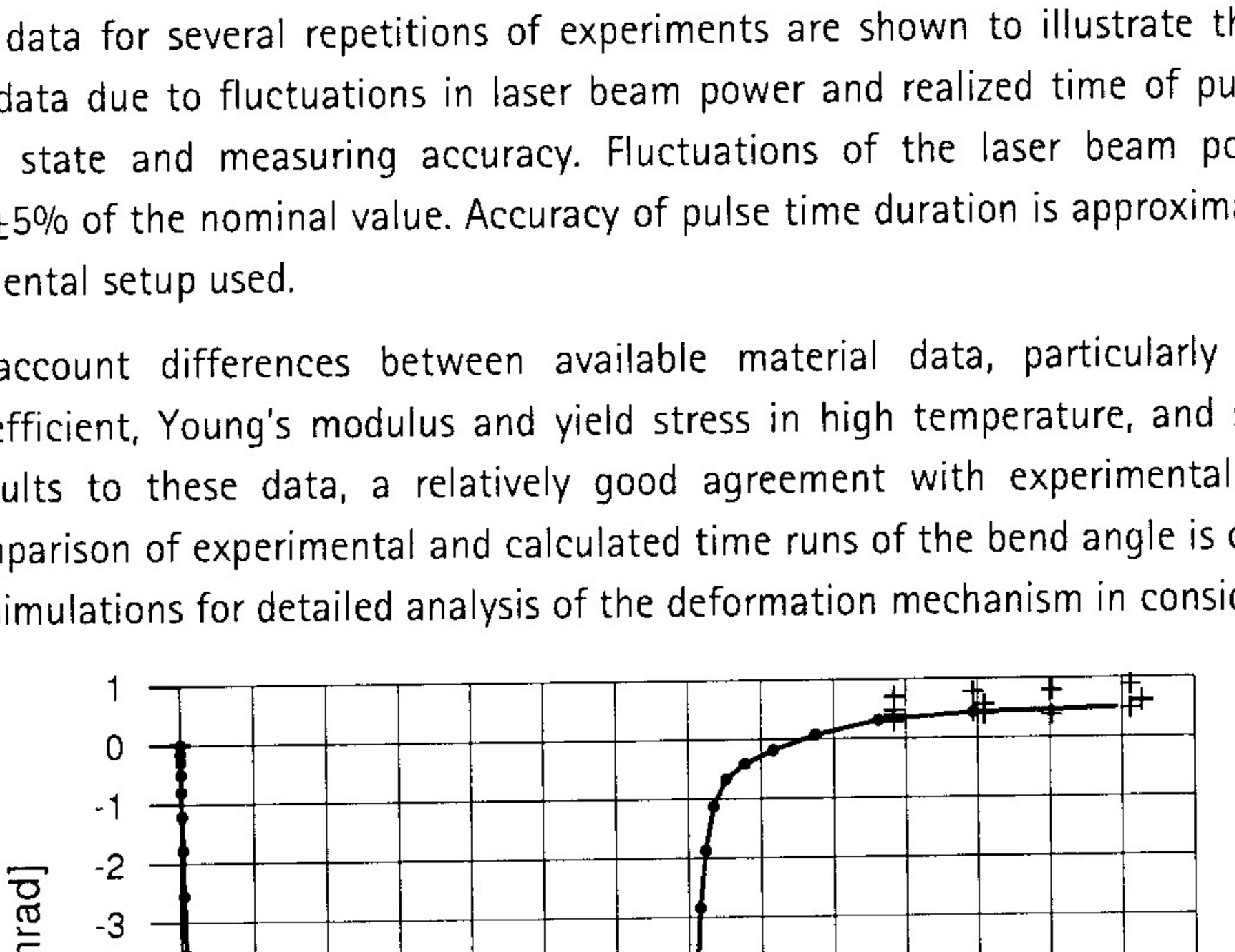

Figure 6: Experimental and numerical bend angle time runs for laser power 90 W and pulse duration 0.35 s

Contour map of the plastic strain component ε_{11}^{pl} at the end of heating stage for laser power 59 W and pulse duration 1.05 s (**figure 7**) reveals compressive deformation in the central region of the sample and tensile deformation in the region closer to the edge of the sample.

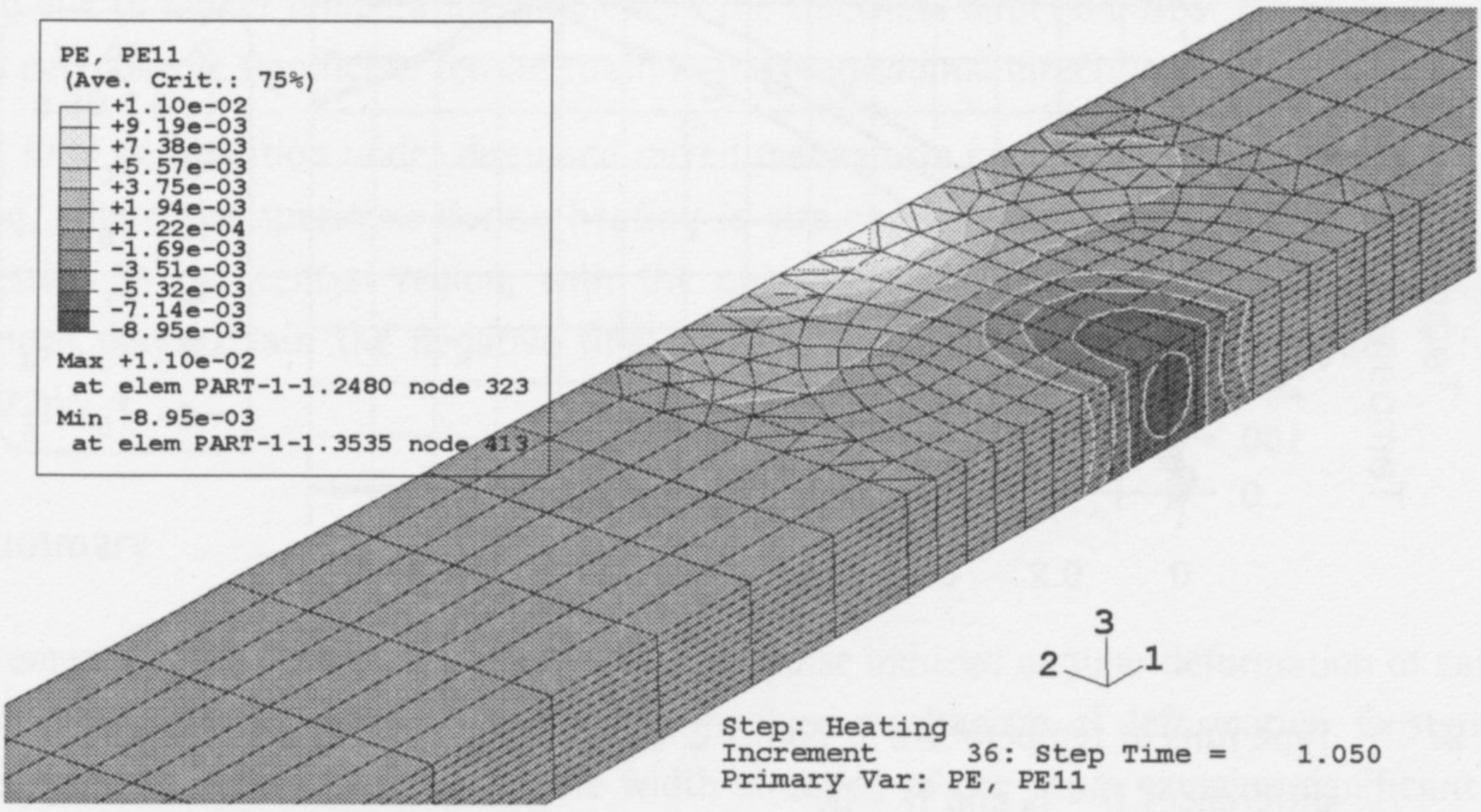

Figure 7: Plastic strain component ε_{11}^{pl} at the end of heating stage for laser power 59 W and pulse duration 1.05 s

Figure 8 presents corresponding time runs of the plastic strain component ε_{11}^{pl} at point C located in the center of the laser spot (see **figure 4a**) and at point E located on the edge of specimen. Plastic deformation on the edge of specimen occurs in an early phase of the heating stage, even earlier than it does in the sample center. The magnitude of plastic elongation on the edge is bigger than the magnitude of upsetting in the center point at the end of laser pulse. During the cooling stage plastic deformation on the edge of specimen quickly drops down, but remains positive.

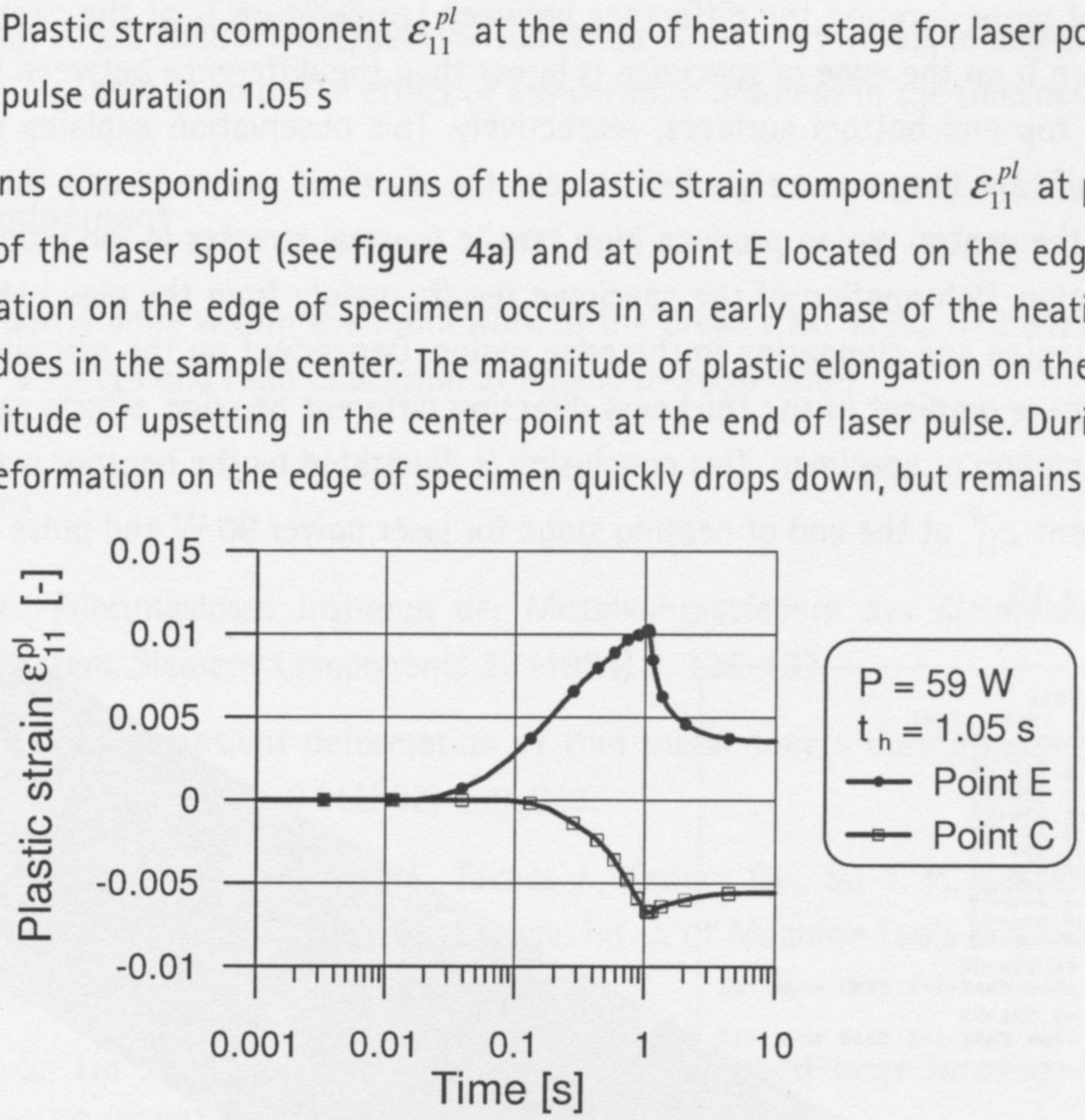

Figure 8: Time runs of plastic strain component ε_{11}^{pl} for laser power 59 W and pulse duration 1.05 s at selected points C and E shown in **figure 4a**

Calculated time runs of temperature at points C, E and point B located on the bottom surface (**figure 4a**), beneath the point C, are shown in **figure 9**. Temperature gradients in the direction of material thickness and across the width of specimen can be characterized by differences between

temperatures at points C, E and B. Time runs of corresponding temperature differences are also presented in **figure 9**.

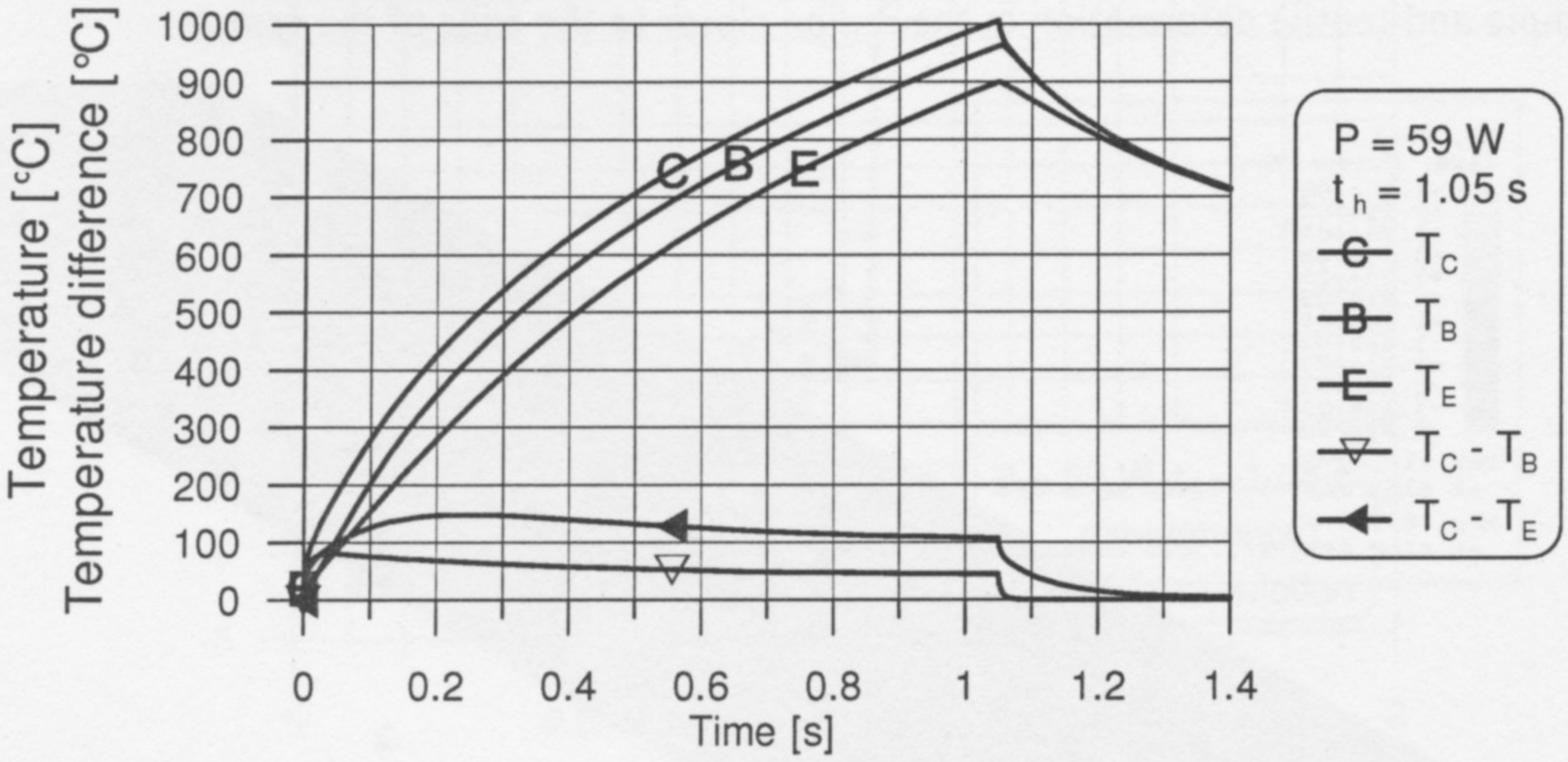

Figure 9: Time runs of temperature at points C, E and B (T_C, T_E, T_B) and temperature differences T_C - T_B and T_C - T_E.

For the most of pulse duration the difference between temperature T_C at the center of laser spot and temperature T_E on the edge of specimen is larger than the difference between temperatures T_C and T_B on the top and bottom surfaces, respectively. This observation explains behavior of the specimen. Significant temperature gradient across the width of specimen and thermal expansion of material in the central region produce high tensile thermal stresses in longitudinal direction 1 in the edge region. Deformation of the specimen results mainly from the play between upsetting in the central region and elongation in the edge region. Dependent on the magnitude and history of the temperature gradient in the thickness direction different bending effects can contribute to the final deformation of specimen. This conclusion is illustrated by the contour map of the plastic strain component ε_{11}^{pl} at the end of heating stage for laser power 90 W and pulse duration 0.35 s, shown in **figure 10**.

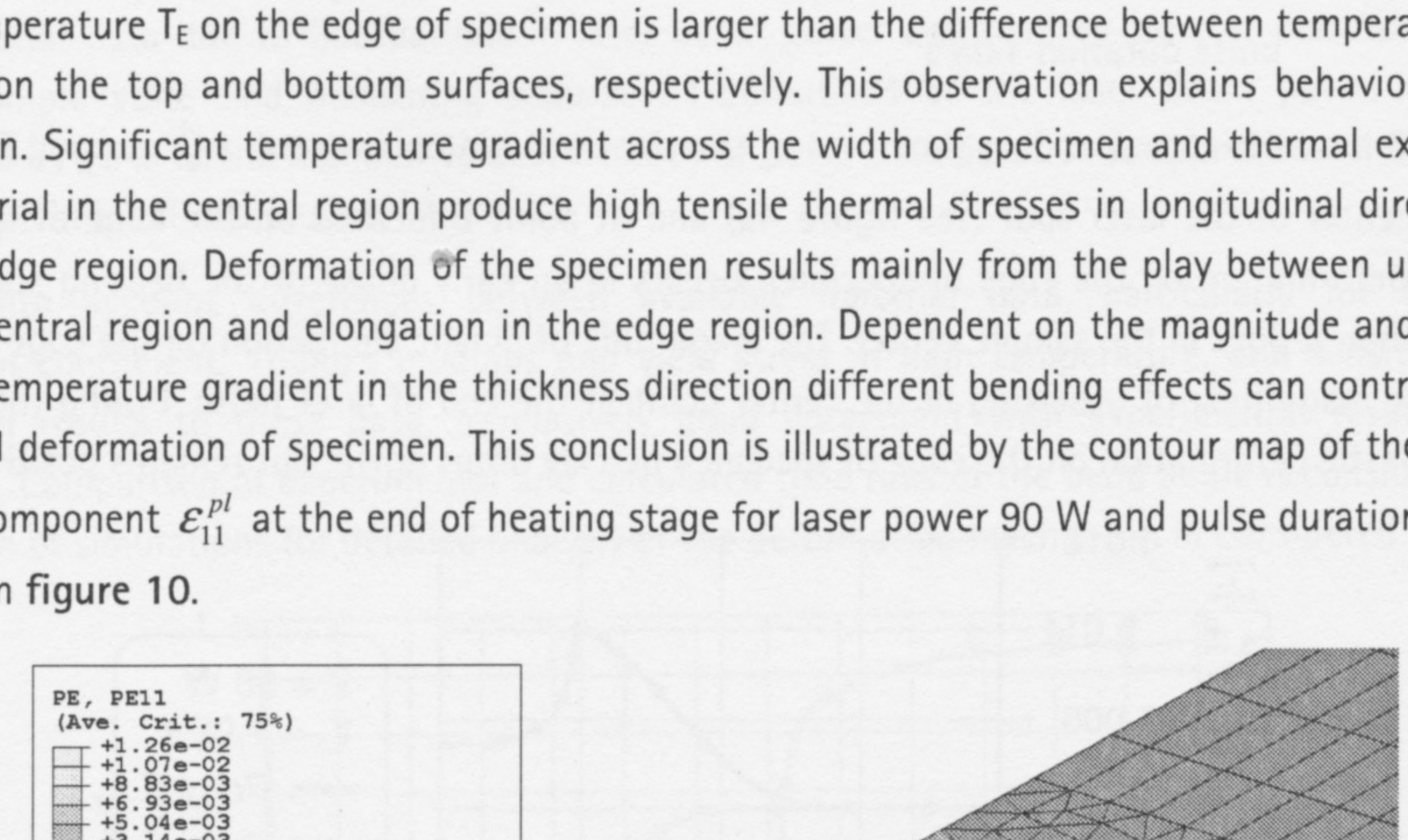

Figure 10: Plastic strain component ε_{11}^{pl} at the end of heating stage for laser power 90 W and pulse duration 0.35 s

Shorter pulse duration with increased laser power, in comparison with case previously discussed, favors temperature gradient mechanism contribution in the deformation. The distribution of strain ε_{11}^{pl} in the central cross-section, along the plane of symmetry of specimen, indicates increased bending due to higher temperature gradient in the thickness direction. Near the edge of specimen we still can observe significant tensile strain in the longitudinal direction.

In fact, final deformation under discussed mixed mechanism can sometimes result from a kind of buckling, where the specimen during heating is strained by tension in the edge region and by compression in the central region, with the opposite stress distribution during cooling. Such mechanism may explain the negative final angular deformation observed in **figure 3** for laser power 72 W.

4 Summary

Measurements and numerical simulations of laser pulse induced angular deformation of cantilever stainless steel beams allowed analysis of the involved mechanism of deformation. Existence of a considerable temperature gradient in the width direction of the beam explains significant tensile plastic deformation in the edge region. Final angular deformation of considered thin beams locally heated with long pulses results from material upsetting in the central region and elongation in the edge region, with contribution of the effect of temperature gradient in the thickness direction.

5 Acknowledgement

This work was partly done within the framework of the project No. N503 012 31/1668 funded by the Ministry of Sciences and High Education of Poland in 2006-2009.

6 References

[1] Steiger E., Führungsloses Justieren der Mittelkontaktfedern des Kleinrelais D2 in einem Pulslasersystem. Siemens Components 22 (1984) 3, 135-137.

[2] Lee K.-C., Lin J., Transient deformation of thin metal sheets during pulsed laser forming. Optics & Laser technology 34 (2002) 639-648.

[3] Wang X. F., Chen G. N., Hu Sh. G., Takacs J., Krallics Gy., Su Y. P., Research on dynamic micro-deformation under laser point source. Int. J. of Machine Tools and Manufacture, Vol. 45, Issue: 12-13, 2005, 1515-1522.

[4] Hsieh H.-S., Lin J., Laser-induced vibration during pulsed laser forming. Optics & Laser Technology 36 (2004) 431-439.

[5] Zhang X. R., Xu X., Finite Element Analysis of Pulsed Laser Bending: The Effect of Melting and Solidification, Transactions of ASME, Journal of Applied Mechanics, Vol. 71, 2004, pp. 321-326.

[6] Zhang X. R., Xu X., Laser bending for high-precision curvature adjustment of microcantilevers. Appl. Phys. Lett. 86, 021114 (2005).

[7] Carslaw H. S., Jaeger J. C., Conduction of Heat in Solids. Oxford University Press, 1946.

[8] Arnet H., Vollertsen F., Extending Laser Bending for the Generation of Convex Shapes. J. of Engineering Manufacture, Vol. 209, No B5 (1995), 433-442.

[9] Li W., Yao Y. L., Laser Forming with Constant Line Energy. Int. J. Advanced Manufacturing Technology, Springer-Verlag, Vol. 17, 2001, 196-203.

[10] Vollertsen F., Mechanisms and Models for Laser Forming. Proc. of LANE '94, Eds.: M. Geiger, F. Vollertsen. Meisenbach-Verlag, Bamberg (1994), 345-360.

[11] Mucha Z., Widłaszewski J., Cabaj M., Grado R., Surface temperature control in laser forming. Archives of Thermodynamics, Vol. 24 (2003), No. 2, 89-105.

[12] Frolov W. W., Vinokurov V. A., Volczenko W. N., Parachin W. A., Arutionowa I. A., Theoretical foundations of welding. High School Publishing House, Moscow 1970 (in Russian).

[13] Inoue Y., Kikuchi M., Present and Future Trends of Stainless Steel for Automotive Exhaust System. NIPPON STEEL TECHNICAL REP. 88, 2003.

[14] Colombier L., Hochmann J., Stainless and Heat-Resisting Steels. Silesia Publishing House, 1964 (Polish translation).

[15] Kim C. S., Thermophysical properties of stainless steels. Technical Report ANL-75-55. Argonne National Laboratory, Argonne, Ill., 1975, 1-24.